CORROSION SCIENCE AND TECHNOLOGY, Vol.16, No.4(2017), pp.175~182
[Research Paper]
pISSN: 1598-6462 / eISSN: 2288-6524
DOI: https://doi.org/10.14773/cst.2017.16.4.175

# Influence of Carbon Fiber on Corrosion Behavior of Carbon Steel in Simulated Concrete Pore Solutions

**Yuming Tang, Yuchao Dun, Guodong Zhang, Xuhui Zhao, and Yu Zuo†**

*Beijing Key Laboratory of Electrochemical Process and Technology for Materials, Beijing University of Chemical Technology, Beijing 100029, China*

(Received February 11, 2017; Revised February 11, 2017; Accepted August 17, 2017)

Galvanic current measurement, polarization curves, electrochemical impedance spectroscopy and weight loss test were used to study the corrosion behavior of carbon steel before and after carbon fibers coupling to the carbon steel in simulated concrete pore solutions, and the film composition on the steel surface was analyzed using XPS method. The results indicate that passive film on steel surface had excellent protective property in pore solutions with different pH values (13.3, 12.5 and 11.6). After coupling with carbon fibers (the area ratio of carbon steel to carbon fiber was 12.31), charge transfer resistance $R_{ct}$ of the steel surface decreased and the $Fe^{3+}/Fe^{2+}$ value in passive film decreased. As a result, stability of the film decreased and the corrosion rate of steel increased. Decreasing of the area ratio of steel to carbon fiber from 12.3 to 6.15 resulted in the decrease in $R_{ct}$ and the increase in corrosion rate. Especially in the pore solution with pH 11.6, the coupling leads the carbon steel to corrode easily.

***Keywords:*** *simulated concrete pore solution, carbon steel, carbon fiber, galvanic corrosion*

## 1. Introduction

Carbon fiber reinforced concrete (CFRC) has many excellent physical and chemical properties [1-4], compared with the conventional reinforced concrete structural materials. Because of the good electrical conductivity of carbon fiber (CF), CFRC could achieve some special requirements, such as stress monitoring, temperature monitoring, self-sensing of strain and electromagnetic shielding [5,6]. Basically, carbon fiber materials have been used in reinforced concrete structures in two ways. One is mixing some short carbon fibers into reinforced concrete or part of concrete cover, so as to achieve excellent enhancement effects [7,8]. Another way is to use carbon fiber-reinforced polymer composites (CFRP) or carbon fiber laminates (sheets) to strengthen or repair the reinforced concrete structure [9,10]. No matter in which way, it is likely for fibers to contact with reinforcing steels in concretes. Because the potential of carbon fiber is more positive than that of the steel, the contact between these two materials will form a galvanic couple, then as the anode the steel might suffer an accelerated corrosion.

Some researchers have studied the galvanic corrosion between carbon fibers and steel in simulated seawater and antifreeze solutions. The results showed the existence of galvanic corrosion if the exposed conductive carbon fiber in the reinforced composite material contacts with steels, and steel corrosion could be aggravated by galvanic action [11-13]. Some researchers pointed out that the galvanic action could also accelerated the degradation of carbon fiber-reinforced polymer composites [14]. So, it has been suggested to use a thicker non-conductive layer (such as epoxy film or a GFRP sheet) to isolate the carbon and the steel to reduce the possibility of galvanic corrosion and slow the corrosion rate of the steel [15]. However, few materials could retain their insulating properties for more than a few years due to wear, chemical breakdown or electrolyte adsorption [16]. If the steel rebar is coated but damaged, the corrosion rate of the steel would increase ten times compared to CFPR-uncoated bar couples [14]. Generally, within the high alkaline environment of concrete (pH 12.5~13.3), reinforcing steel is well protected against corrosion by a passive oxide film formed on the surface. However, the concrete carbonation causes the depassivation of steel. When the pH of concrete pore solution drops to 11.5, the stability of the passive film on carbon steel surface is difficult to maintain [17]. Many researchers have studied the effect of concrete pH on the corrosion behavior of steels [18]. But under the circumstance when carbon fibers contacts with steel in concrete

† Corresponding author: zuoy@mail.buct.edu.cn

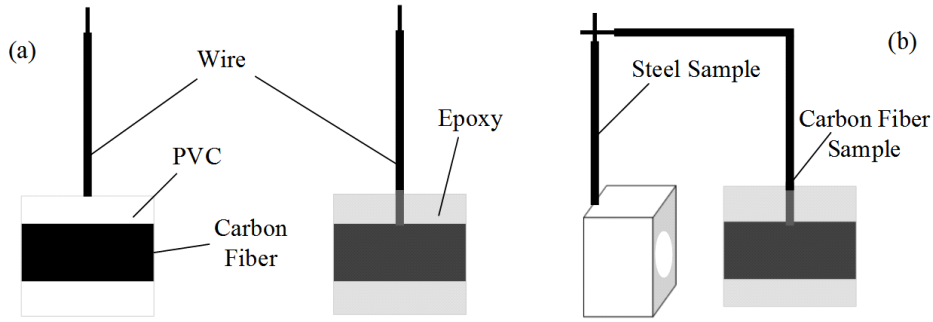


**Fig. 1 Schematic diagrams of electrochemical test samples: (a) CF sample; (b) steel sample with CF sample coupling.**

environment, the effect of pH variation on the corrosion of carbon steel was rarely reported. In this paper, the effect of coupling carbon fibers on the surface passivation and the electrochemical behavior of carbon steel in simulated concrete pore solutions with three pH values from high alkaline to slight carbonation conditions were investigated. The influence of coupling area of carbon fibers on the electrochemical behavior of carbon steel was also investigated.

## 2. Experimental methods

### 2.1 Materials

The study material was Q235 carbon steel with the chemical composition (wt%): 0.37% C, 0.16% Si, 0.32% Mn, 0.053% S, 0.026% P, and the balance Fe. Three types of simulated concrete pore solutions (SPSs) were selected to present pore solutions within a high alkaline, alkaline and slightly carbonated concrete environment [19]. The chemical compositions of the SPSs were 3.7 g/L NaOH + 10.5 g/L KOH + 2.0 g/L $Ca(OH)_2$ (pH 13.3), 2.0 g/L $Ca(OH)_2$ (pH 12.5), 0.0833 g/L NaOH + 0.233 g/L KOH (pH 11.6), respectively.

The steel rebar with 1 cm diameter was cut into 1 cm length as steel sample. One surface of the sample was abraded with emery papers up to 1000 grit, rinsed in deionized water and degreased with acetone, finally dried in warm air. The sample was covered with epoxy resin, leaving an area of 0.4 $cm^2$ exposed to the test solution. A bunch of carbon fibers were entangled around the PVC plastic sheet and the back side of the PVC sheet was encapsulated with epoxy to make the carbon fibers contact with copper wire. The lengths of the exposed carbon fibers were 5 cm and 10 cm, respectively. The schematic is shown in Fig. 1a. Steel sample with carbon fibers coupling was prepared by connecting carbon fiber sample and steel sample with copper wire, as shown in Fig. 1b.

The size of carbon steel sample for weight loss test was 15 mm × 10 mm × 2 mm. The steel sheet was punched on one end. The steel surface was cleaned with emery papers up to 1000 grit and then rinsed in deionized water and acetone. The sample with carbon fibers coupling was prepared by passing through the punched hole with a bunch of carbon fibers.

The carbon fiber used in the test was CCF300 3K carbon fiber (China). 3K meant 3000 pieces carbon fiber in each bunch. Carbon fibers were PAN based, with tensile strength of 3800-4100 MPa and tensile modulus of 221-239 GPa. The diameter of carbon fiber was 7 μm. The surface area per unit length for each bunch was 6.5 $cm^2$/cm. The amount of carbon fibers in the test was represented by the length of a bunch of carbon fibers.

### 2.2. Measurement techniques

#### 2.2.1 Electrochemical measurements

The polarization measurement was carried out with a CS350 electrochemical test system (Wuhan Corrtest Instrument Co., China). The polarization test started from the open circuit potential and deviated in the anodic direction at a scan rate of 0.6 mV/s. The electrochemical impedance (EIS) test was performed at open circuit potential by a Parstat 2273 electrochemical test system (Princeton). The amplitude of the AC voltage signal was 5 mV and the frequency varied between $10^{-2}$ and $10^5$ Hz. The electrochemical tests were conducted under room temperature using a three-electrode system with the samples as working electrode, a saturated calomel electrode (SCE) as reference electrode and a platinum electrode as the counter electrode. Before the test, steel samples were all pre-passivated in SPSs for two hours.

Galvanic current test was employed with the CS350 electrochemical test system. The steel sample and carbon fiber sample were connected with WE2 and WE1, respectively.

#### 2.2.2 Weight loss test

The steel sample and the steel sample with carbon fibers coupling were immersed in the simulated pore solutions

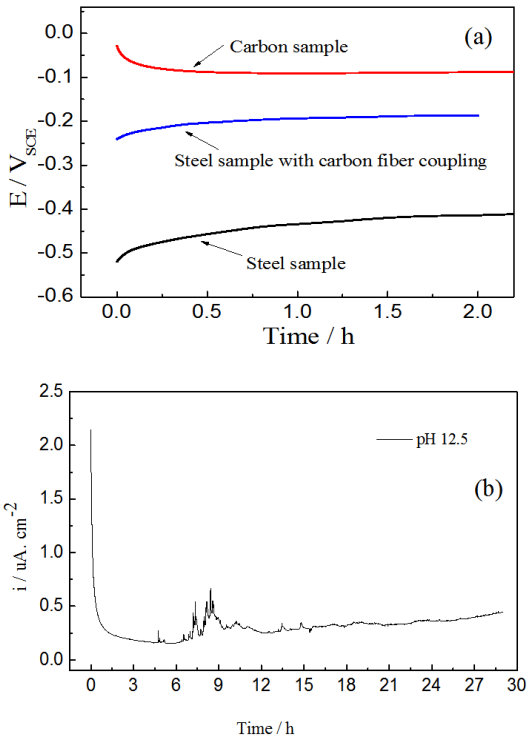


**Fig. 2 Open circuit potential-time curves (a) and galvanic current-time curves (b) for samples in SPS (pH 12.5).**

for 21 days, and then the steel surface was cleaned using a 20% HCl + 5% methenamine solution if there was corrosion products covered. The metallographic microscope was used to observe the surface morphology and the corrosion rate was calculated. The surface area of the steel was 400 $mm^2$. After coupling with 5 cm and 10 cm long carbon fibers, the corresponding area ratio of the steel to carbon fibers was 12.31 and 6.15, respectively.

### 2.2.3 Surface Analysis

The chemical composition of the surface film on the steel surface was analyzed by X-ray photoelectron spectroscopy (Model ESCALAB 250, ThermoFisher Scientific, USA). The surface area ratio of steel to carbon fibers was the same as that for weight loss test.

## 3. Results and Discussion

### 3.1 The potentials monitoring and galvanic current measurements between carbon fibers and the steel

The open circuit potentials of steel sample, carbon fibers sample and steel sample coupling with carbon fibers were monitored in the pH 12.5 SPS, and the galvanic current measurements were carried out for the coupling sample. Fig. 2 shows the results. As seen in Fig. 2a, the

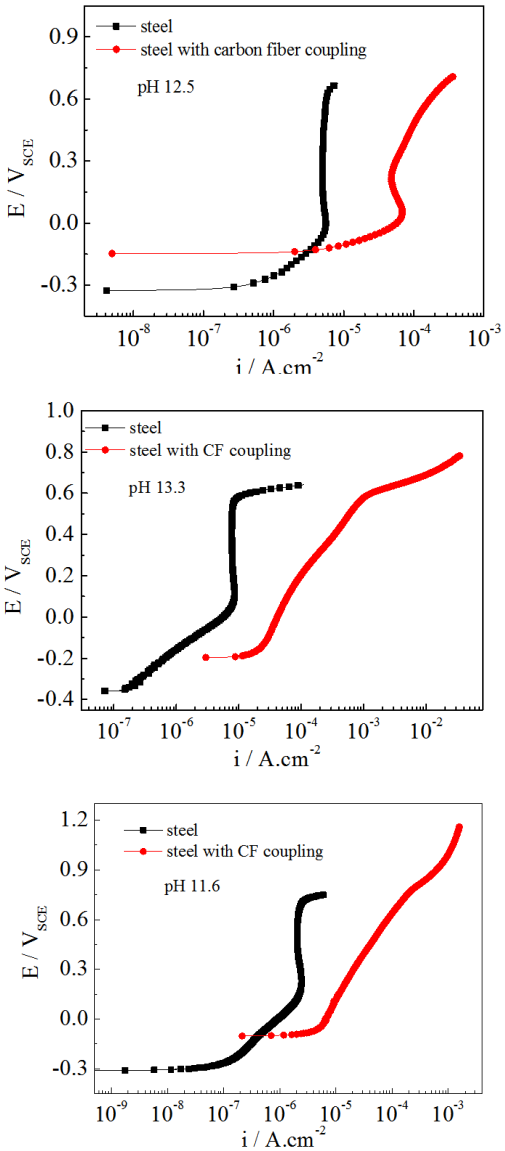


**Fig. 3 Anodic polarization curves of the steel samples before and after coupling with CF in three SPSs.**

potentials of three types of samples were all towards stability after immersion for 2 h. Before coupling, the steel potential was about -410 mV and the potential for carbon fibers maintained at -90 mV. After coupling, the system reached a mixed potential around -190 mV, which was more positively than the steel before coupling. So, the steel would suffer anodic polarization being the anode of the couple. In Fig. 2b, the galvanic current was typically between 0.1 μA/$cm^2$ and 0.3 μA/$cm^2$ with small amplitude of fluctuations occasionally. After the test, no apparent corrosion signs were observed on the steel surface. In the literature [20], less than 0.1 μA/$cm^2$ currents indicate neg-

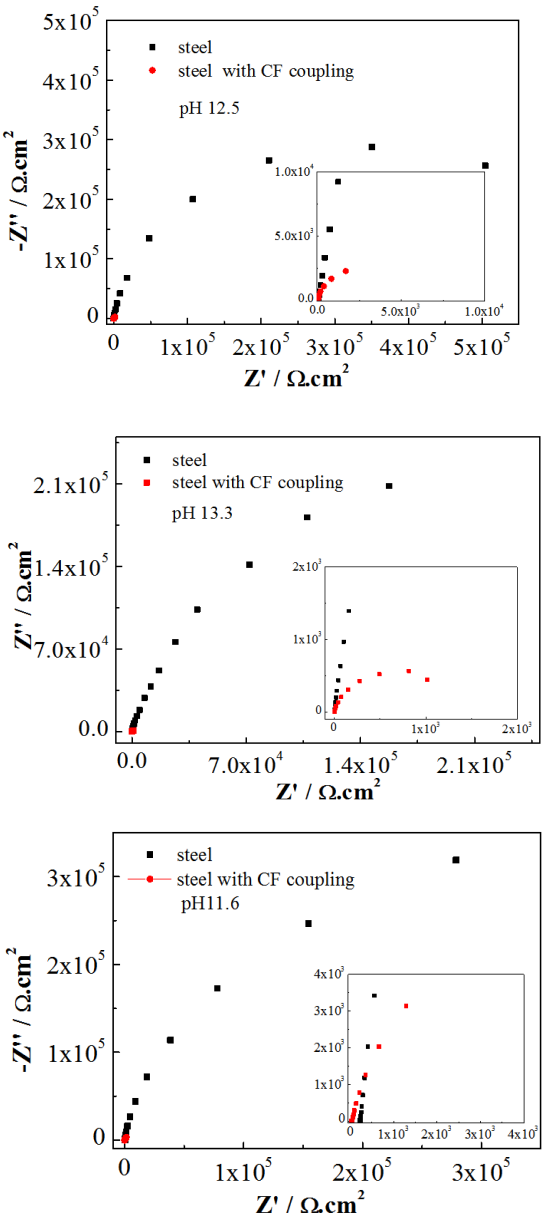


**Fig. 4 Nyquist plots of steel samples before and after CF coupling in three SPSs.**

ligible corrosion level; more than 1 μA/cm$^2$ indicates high level of corrosion. Hence, the galvanic current probably had some influence on the corrosion of the steel.

### 3.2 The influence of carbon fiber coupling on the polarization and EIS of carbon steel in SPSs

Fig. 3 shows the anodic polarization curves of the steel samples and steel samples with carbon fiber coupling in three types of pore solutions. Before coupling, obvious passive regions were observed on the steel polarization curves in all solutions, which indicated that the steel surface could stay in the passive condition in a wide potential range. After coupling, the corrosion potentials moved positively with no apparent passive region and the corrosion current density increased. This meant that coupling with carbon fibers could decrease the passive property of the steel surface.

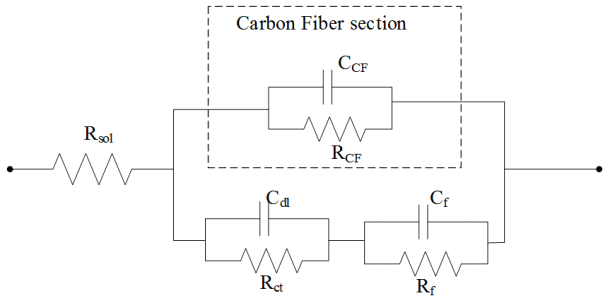


**Fig. 5 Equivalent circuit used to model the EIS plots of steel sample coupling with carbon fibers in pore solution.**

The EIS plots of the carbon steel before and after coupling in pore solutions are illustrated in Fig. 4. Before coupling, an obvious capacitive arc was observed at medium and low frequencies for the steel. After coupling, the radius of the arc reduced apparently, and the impedance at 0.01 Hz frequency ($|Z|_{0.01Hz}$) dropped by two orders of magnitude. The reasons for the drop of the impedance were analyzed. One reason may result from the decrease of the integral resistance of the couple system after coupling with conductive carbon fibers. The other one might due to the decrease of the surface impedance of the steel itself. According to the literature [21], the current transmission in carbon fiber reinforced concrete could be carried in the following three ways: (1) through carbon fibers and cement paste, (2) through mutual overlapped carbon fibers; (3) through the cement paste directly. When carbon fibers and steel are in direct contact in simulated pore solutions, the current is carried mainly by the steel and fibers together. In order to obtain the information of the surface of steel, the EIS data was fitted by an equivalent circuit (Fig. 5). Where $R_s$ is the resistance of solution, $C_{dl}$ and $R_{ct}$ are the double-layer capacitance and the charge-transfer resistance of the steel surface, respectively. $R_f$ and $C_f$ represents the impedance of the compact precipitates layer (such as calcium hydroxide et al.) on the steel film [22]. $R_{CF}$ and $C_{CF}$ are the resistance and capacitance respectively, which are introduced after carbon fibers coupling.

The fitting result is shown in Table.1. It can be seen that, after coupling with carbon fibers, the $R_{ct}$ of steel decreased by 3~4 orders of magnitude and $C_{dl}$ increased by 2~3 orders of magnitude. It could be speculated that

**Table 1 EIS results of the steel samples before and after CF coupling in pore solution (C/$10^{-6}$ F·$cm^{-2}$, R/Ohm·$cm^2$)**

| pH value | samples | $C_{CF}$ | $R_{CF}$ | $C_f$ | $R_f$ | $C_{dl}$ | $R_{ct}$ |
|---|---|---|---|---|---|---|---|
| 12.5 | Steel | — | — | 12.70 | 2032 | 4.92 | $1.44\times10^6$ |
| | After coupling | 110 | $1.16\times10^4$ | 1580 | 13.51 | 5130 | 78 |
| 13.3 | Steel | — | — | 16.01 | $1.08\times10^4$ | 3.75 | $9.82\times10^5$ |
| | After coupling | 22.56 | 2961 | 1957 | 7.11 | 3393 | 117.1 |
| 11.6 | Steel | — | — | 20.84 | $1.85\times10^4$ | 10.09 | $1.47\times10^6$ |
| | After coupling | 31.74 | $2.26\times10^4$ | 1556 | 61.42 | 3129 | 222 |

the changes of $R_{ct}$ and $C_{dl}$ and the parallel connection with carbon fibers were the two main reasons for the decrease of the steel impedance. $R_{ct}$ is the parameter which could reflect the mass transfer ability in the passive film. The lager the $R_{ct}$ value, the better passivation the steel has. The data in Table.1 indicated that in three types of pore solutions, after coupling with carbon fibers, the protective property of the film on steel surface decreased.

For the steel electrode, the capacitance of the passivation film formed on the steel can be simulated by plate capacitor. It can be assumed that the charges are uniformly distributed on the two plates, so the capacitance can be formulated as the following equation:

$$Cdl = \varepsilon S/4\pi kd$$

,where S is the plate area of the parallel plate capacitor, which is the exposed area of carbon steel electrode and ε is the dielectric constant of the film, k is the Boltzmann constant ($1.3806503\times10^{-23}$ J/K), d represents the plate distance of the parallel plate capacitor, which refers to the thickness of the film. Because S and ε are fixed values plus π and k are constants, it could be speculated that d might decrease, which indicated the thickness of film on the steel surface decreasing after coupling with carbon fibers. In addition, the increase in $C_f$ and decrease in $R_f$ values indicated that the amount of the alkaline calcareous precipitates on the steel surface were probably reduced.

### 3.3 Surface composition analysis of the steel before and after coupling in three types of pore solutions

The steel samples before and after carbon fibers coupling were pre-passivated in the pH 12.5 pore solution for 2 h, then taken out and cleaned with alcohol. XPS was performed on the surface of the steel. The spectrum results are shown in Fig. 6. It could be determined that, with the exception of the external standard elements C, the film on the steel surface contained O, Ca and Fe elements with the atomic percentage of 29.08%, 2.81% and 6.87%, respectively (Fig. 6a). Among them, Ca was mainly from the $CaCO_3$ and alkaline compounds precipitates on the steel surface, and O was mainly from the compounds of iron and calcium or water.

According to the literatures [23], the passive film formed on carbon steel in the pH 12.5 pore solution may contain FeOOH, $Fe_2O_3$, FeO and $Fe_3O_4$. Fig. 6b illustrates the typical curve fitting conducted for Fe 2P high resolution XPS spectrum. $Fe^{3+}$ was from FeOOH, $Fe_2O_3$ and $Fe_3O_4$, and $Fe^{2+}$ was in FeO and $Fe_3O_4$. According to the peak parameters of chemical species ($Fe^0 2p_3$ 706.6 ± 0.3 eV, $Fe^{3+}2p_3$ 711 ± 0.4 eV, $Fe^{2+}2p_3$ 709.6 ± 0.3 eV, $Fe_3C$ 707.7 ± 0.4 eV) [23,24], the contents of $Fe^{3+}$ and $Fe^{2+}$ by fitting calculation were 36.1% and 25.4%, respectively. In addition, the Fe content in cementite was 21% and Fe accounted 17%. So, the passive film on the steel surface was mainly composed of $Fe^{3+}$ and some $Fe^{2+}$. The ratio of $Fe^{3+}$ to $Fe^{2+}$ ($Fe^{3+}/Fe^{2+}$) was 1.42. This result was consistent with the result in literatures [23,25], which concluded that the passive film of steel formed in SPS is mainly consists of γ-FeOOH and $Fe_2O_3$ and a small quantity of $Fe^{2+}$.

Fig. 6c shows the XPS spectrum of the steel after coupling with carbon fibers. The atomic percentage of the O, Ca and Fe element was 31.02%, 1.47% and 6.19%, respectively. After coupling, there was a slight decrease of calcium content on the steel surface, indicating the decrease of alkaline precipitates. This was consistent with the results of $C_f$ and $R_f$ in EIS test. Normally, the surface oxidative modification of carbon fibers is a commonly method to increase the surface polarity of fiber and improve its active surface area and oxygen functional groups such as -COOH, -OH, and -CO [26]. The treated carbon fiber can adsorb some metal ions [27,28]. It could be

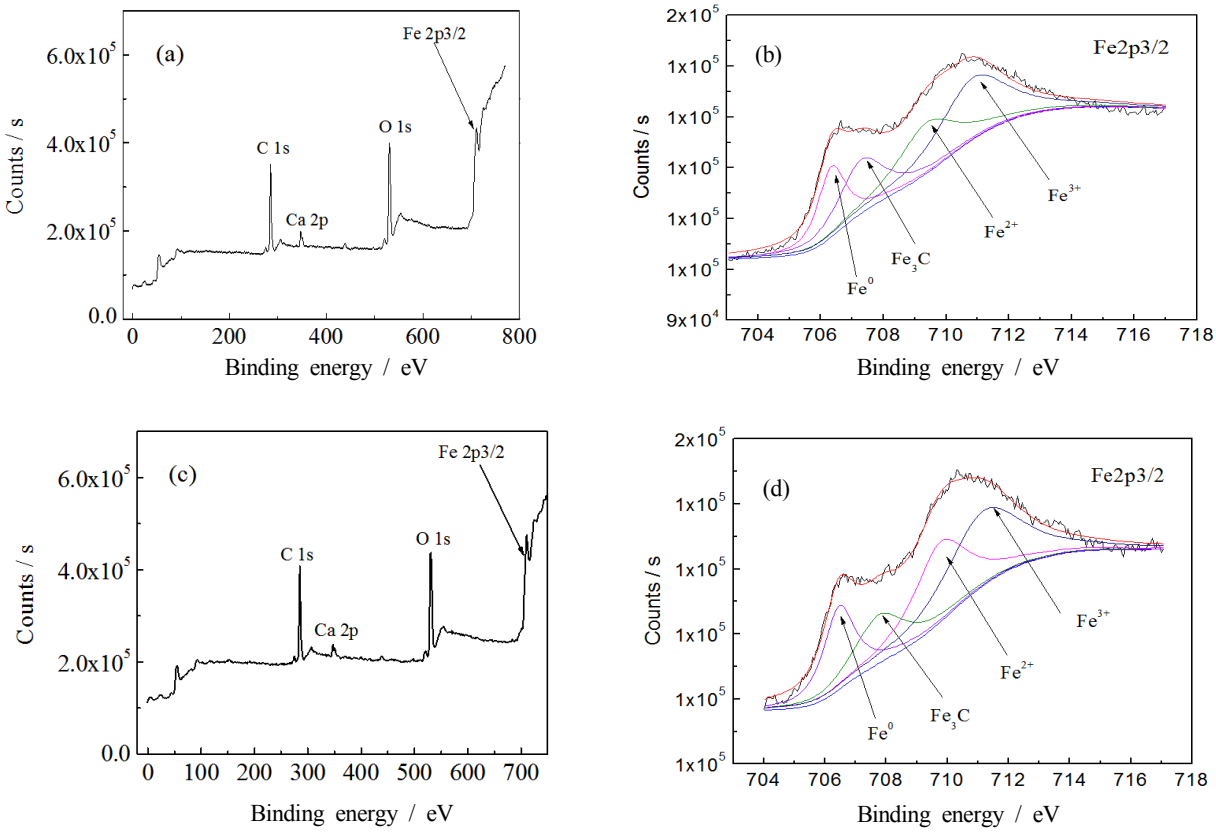


**Fig. 6 XPS spectrum for the steel before and after CF coupling in pH 12.5 SPS: (a), (c)C-survey; (b), (d)-Fe 2p3/2.**

speculated that the decrease of the alkaline precipitates on the steel surface might be due to the adsorptive action of carbon fibers and the reaction between $Ca(OH)_2$ in the solution and the carboxyl on the fiber surface. The fitting result for Fe 2p XPS spectrum in Fig. 6d shows that the content of $Fe^{2+}$ in the passive film was increased. The contents of $Fe^{3+}$ and $Fe^{2+}$ were 37.3% and 28.7%, respectively. It was reported [22,24] that the content of $Fe^{3+}$ and $Fe^{2+}$ can be used to evaluate the protective property of the passive film. The higher ratio of $Fe^{3+}/Fe^{2+}$, the higher content of FeOOH and $Fe_2O_3$ in the film, meaning the better stability and protective performance of the film. Conversely, the lower ratio, the higher content of FeO and $Fe_3O_4$, indicating the worse stability and poorer protective performance the film has. After coupling, the $Fe^{3+}/Fe^{2+}$ ratio dropped from 1.42 to 1.3, reflecting the decrease of the film protective property. This agreed with the above electrochemical test results.

The surface of the steel formed in the pore solutions with pH 13.3 and 11.6 were analyzed by XPS. (The spectra are not shown). The calculated ratio of $Fe^{3+}/Fe^{2+}$ showed that the ratios deceased after the steel coupled with carbon fiber (from 2.1 or 1.18 decreased to 1.47 or 0.57, respectively), indicating the decrease of the film stability. This is similar to the result in pH 12.5 pore solution.

### 3.4 Influence of the coupling volumes of CF on the electrochemical behaviour and surface composition of carbon steel

Fig. 7 shows the anodic polarization curves of the steel samples coupled with a bunch of 5 cm long fibers and

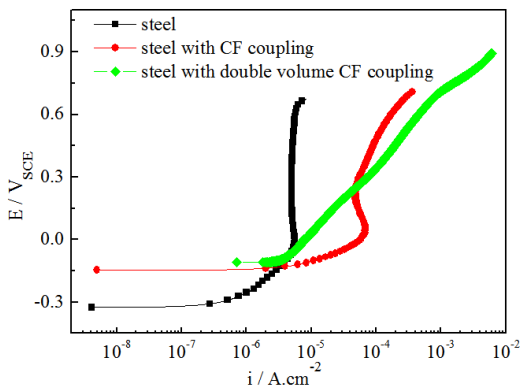


**Fig. 7 Anodic polarization curves of steel samples with various volumes of CF coupling in pH 12.5 SPS.**

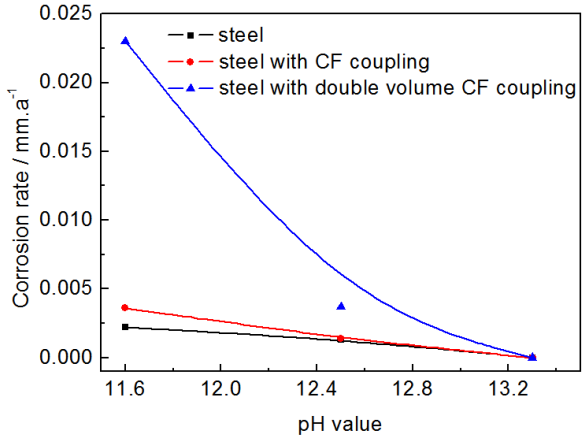


**Fig. 8 Corrosion rates of the steel with various volume amounts of CF coupling in three SPSs by weight-loss test.**

10 cm long fibers separately in the pore solution (pH 12.5). The according area ratio of carbon steel to carbon fiber was 12.31 and 6.15, respectively. It can be seen that after the area of carbon fibers increased, the corrosion potential increased, while the polarization curve showed apparent active characteristic indicating the decrease of the corrosion resistance of steel.

Fig. 8 shows the corrosion rates of the steel before and after coupling with different areas of carbon fibers, which were calculated by 21 d weight loss test result in the pore solutions with pH value of 11.6, 12.5 and 13.3, respectively. It can be seen clearly that the corrosion rate of the steel was very low (0.0022 mm/yr, 0.0013 mm/yr and 0, respectively), and decreased with the increase in pH value, though the amplitude of the variation was very small. After coupling, the corrosion rate increased a little ($3.6 \times 10^{-3}$ mm/yr, $1.4 \times 10^{-3}$ mm/yr and 0) and decreased with the increase of the solution pH too. Under the same pH condition, the corrosion rate increased with the coupling area doubled. Among of them, in pH 11.6 pore solution, the increase amplitude of the corrosion rate was the biggest, and after the test visible corrosion was observed on the steel surface. With the pH value increasing (to 12.5 and 13.3), the influence of the CF area doubled on the steel corrosion became smaller. It is worth to note that in the pH 13.3 solution, the corrosion rates of the steels were almost zero, which indicated that coupling with carbon fibers had little influence on the corrosion of the steel in the high alkaline solution (pH 13.3). The difference between the weight loss test and the electrochemical tests results probably were caused by the difference of the tests. In addition, another probable reason was the regardless of the carbon fibers area influence during the electrochemical data processing.

## 4. Conclusions

(1) In the three types of simulated pore solution (pH 13.3, 12.5 and 11.6), the surface of the carbon steel could maintain good passivation state. After coupling with carbon fibers (the area ratio of carbon steel to carbon fiber was 12.31), the open circuit potential of the steel shifted positively, the impedance of the steel surface decreased, and the corrosion enhanced. The galvanic current from the steel and carbon fibers couple had some influence on the corrosion of the steel. XPS result showed that the ratio of $Fe^{3+}/Fe^{2+}$ in the passive film decreased and therefore the film stability decreased.

(2) The weight loss result reviewed the accelerate effect on the corrosion of steel by the increase of the coupling area of carbon fiber coupling. As the solution pH decreasing, the amplitude of the corrosion rate increased. Especially in slight carbonation solution (pH 11.6), the acceleration effect became obvious, which manifested by the apparent corrosion signs observed on the steel surface after immersion in the solution for 21 days.

## Acknowledgements

The authors would like to thank the National Natural Science foundation of China (Contract 51210001) for support to this work.

## References

1. J. G. Zoran, A. T. C. Gordana, S. R. Nenad, and M. D. Iva, *Constr. Build. Mater.*, **27**, 305 (2012).
2. S.-J. Park and M.-K. Seo, *Mat. Sci. Eng.* A, **366**, 348 (2004).
3. C. Desmettre and J.-P. Charron, *Cement Concrete Res.*, **42**, 945 (2012).
4. J. Y. Hou and D. D. L. Chung, *Cement Concrete Res.*, **27**, 649 (1997).
5. S. Wen and D. D. L. Chung, *Cement Concrete Res.*, **31**, 665 (2001).
6. J. Wu and D. D. L. Chung, *Carbon*, **40**, 445 (2002).
7. Z.-Q. Shi and D. D. L. Chung, *Cement Concrete Res.*, **29**, 435 (1999).
8. S. Ivorra, P. Garcés, G. Catala, L. G. Andio, and E. Zornoza, *Mater. Design*, **31**, 1553 (2010).
9. X.-G. Wang, W.-P. Zhang, W. Cui, and F. H. Wittmann, *Cement Concrete Comp.*, **33**, 513 (2011).
10. A. H. Al-Saidy and K. S. Al-Jabri, *Compos. Struct.*, **93,** 1775 (2011).
11. M. Tavakkolizadeh and Hamid Saadatmanesh, *J. Compos. Constr.*, **5**, 200 (2001).

12. X. W. Guo, *Dev. Appli. Mater.*, **13**, 16 (1998).
13. A. A. Torres-Acosta, A. A. Sagues, and R. Sen, *Proc. NACE Conf.*, Paper No.98648, Houston, TX (1998).
14. A. A. Torres-Acosta and R. Sen, *J. Appl. Electrochem.*, **35**, 529 (2005).
15. D. Schnerch, K. Stanford, E. Sumner, and S. Rizkalla, *Proc. International Symposium on Bond Behaviour of FRP in Structures Conf.,* pp. 435-444, Hong Kong, China (2005).
16. F. E. Sloan and J. B. Talbot, *Corrosion*, **48**, 830 (1992).
17. A. Bentur, N. Berke, and S. Diamond, *Steel corrosion in concrete: fundamentals and civil engineering practice*, 2nd ed., pp. 1-208, CRC Press, London, UK (2005).
18. B. Huet, V. L'Hostis, F. Miserque, and H. Idrissi, *Electrochim. Acta*, **51**, 172 (2005).
19. H. Yu, K.-T. K. Chiang, and L. Yang, *Constr. Build. Mater.*, **26**, 723 (2012).
20. ASTM-1065, C. Andrade, M. C. Alonso, and J. A. Gonzalez, An initial effort to use the corrosion rate measurements for estimating rebar durability. Corrosion Rates of Steel in Concrete, pp. 29-37, Philadelphia (1990).
21. B. Chen, W. Yao, and K.-R. Wu, *Mat. Sci. Eng.*, **19**, 76 (2001).
22. S. J. Ford, J. D. Shane, and T. O. Mason, *Cement Concrete Res.*, **28**, 1737 (1998).
23. P. Ghods, O. B. Isgor, J. R. Brown, F. Bensebaa, and D. Kingston, *Appl. Surf. Sci.*, **257**, 4669 (2011).
24. D. S. Petrovic and D. Mandrino, *Mater. Charact.*, **62**, 503 (2011).
25. W. Ying, Y. X. Shi, and B. M. Wei, *J. Chinese Soc. Corros. Protection*, **18**, 107 (1998).
26. G. Zhang, S. Sun, D. Yang, J. P. Dodelet, and E. Sacher, *Carbon*, **46**, 196 (2008).
27. Z. R. Yue, W. Jiang, L. Wang, H. Toghiani, S. D. Gardner, and C. U. Pittman Jr., *Carbon*, **37**, 1607 (1999).
28. J. W. Shim, S. J. Park, and S. K. Ryu, *Carbon*, **39**, 1635 (2001).